



OPEN Examining transfer of TERT to mitochondria under oxidative stress

Dmitrii Burkatovskii¹, Andrey Bogorodskiy¹, Ivan Maslov¹, Olga Moiseeva^{1,2}, Roman Chuprov-Netochin¹, Ekaterina Smirnova¹, Nikolay Ilyinsky¹, Alexey Mishin¹, Sergey Leonov^{1,3}, Georg Bueldt¹, Valentin Gordeliy¹, Thomas Gensch⁴ & Valentin Borshchevskiy¹✉

The primary role of telomerase is the lengthening of telomeres. Nonetheless, emerging evidence highlights additional functions of telomerase outside of the nucleus. Specifically, its catalytic subunit, TERT (Telomerase Reverse Transcriptase), is detected in the cytosol and mitochondria. Several studies have suggested an elevation in TERT concentration within mitochondria in response to oxidative stress. However, the origin of this mitochondrial TERT, whether transported from the nucleus or synthesized *de novo*, remains uncertain. In this study, we investigate the redistribution of TERT, labeled with a SNAP-tag, in response to oxidative stress using laser scanning fluorescence microscopy. Our findings reveal that, under our experimental conditions, there is no discernible transport of TERT from the nucleus to the mitochondria due to oxidative stress.

Keywords TERT, Protein transport, Mitochondria, Oxidative stress, SNAP-tag

The primary role of telomerase is the extension of telomeres, repetitive DNA sequences at the ends of chromosomes of eukaryotic cells. Telomeres shorten with each cell division, and when they reach a critically short length, the cell loses capacity for further division. Telomerase counteracts this shortening and effectively eliminates the constraints on cell division imposed by telomere shortening¹.

Telomerase is a ribonucleoprotein complex encompassing a catalytic protein subunit, TERT (Telomerase Reverse Transcriptase), and an RNA template for the synthesis of telomeric repeats, TERC (Telomerase RNA Component). Beyond their central role in telomere length regulation, TERT and TERC exhibit distinct functions independent of each other². For instance, TERC contributes to the protection of T-cells against apoptosis³, safeguards neurons from oxidative stress⁴, and takes part in inflammatory responses⁵. TERT extratelomeric functions include gene expression regulation in several pathways⁶, as well as RNA-dependent RNA polymerase activity in conjunction with the RNA component of mitochondrial RNA Processing endoribonuclease⁷. TERT interacts with mitochondrial tRNA and the 5.8 S ribosomal subunit rRNA⁸.

Many of TERT's telomerase-independent functions appear to be closely linked to mitochondria. The presence of TERT in mitochondria is substantiated by its Mitochondrial Targeting Sequence (MTS) on the N-terminus and confirmed via fluorescence microscopy imaging experiments⁹. Biochemical studies involving the analysis of mitochondrial lysate fractions suggest that within mitochondria, TERT is primarily located within the matrix, where it interacts with mitochondrial DNA (mtDNA)^{8,10}.

The impact of TERT on mtDNA in response to cellular oxidative stress has gathered significant attention. Existing research presents contradictory findings, with some studies suggesting that TERT intensifies oxidative stress-induced damage to mtDNA^{9,11}, while others propose a protective role for TERT in this context^{8,10,12,13}. In both scenarios, it is evident that TERT is intricately involved in the cellular response to oxidative stress.

This response involves TERT redistribution within the cell. Oxidative stress triggers the export of TERT from the nucleus^{12–14} and an increase in its levels within mitochondria^{12,13,15}. This mechanism seems to have a posttranslational nature, as the nuclear export of TERT under oxidative stress involves its phosphorylation at tyrosine 707 by Src kinase¹⁴.

¹Moscow Institute of Physics and Technology (MIPT), 9 Institutsky lane, Dolgoprudny 141700, Russian Federation.

²G.K. Skryabin Institute of Biochemistry and Physiology of Microorganisms, Federal Research Center "Pushchino Scientific Center for Biological Research of the Russian Academy of Sciences", 5 Prospekt Nauki, Pushchino 142290, Russian Federation. ³Institute of Cell Biophysics, Russian Academy of Sciences, Institutskaya st., Pushchino 142290, Russian Federation. ⁴Laboratory for Photochemistry and Spectroscopy, Division for Molecular Imaging and Photonics, Department of Chemistry, KU Leuven, 3001 Leuven, Belgium. ✉email: borshchevskiy.vi@phystech.edu

A definitive link between the nuclear export of TERT under oxidative stress and the simultaneous elevation of its levels within mitochondria remains elusive. In this study, we investigate whether the mature TERT that exits the nucleus during oxidative stress subsequently translocates to the mitochondria or if mitochondrial TERT is synthesized *de novo*. To explore this, we fluorescently labeled TERT with a SNAP-tag and monitored its redistribution in transfected HeLa cells under oxidative stress induced by adding hydrogen peroxide (H₂O₂) to the cell medium. We employed two experimental approaches: the first involved single fluorescent staining of TERT before the induction of oxidative stress to detect potential transport from the nucleus to mitochondria, while the second approach involved staining TERT before and after the induction of oxidative stress, intended to identify not only transport but also the synthesis of new TERT into mitochondria.

Results

TERT transport from the nucleus into mitochondria under oxidative stress

Two main hypotheses explain how TERT appears in the mitochondria upon oxidative stress: TERT is either transported from the nucleus or synthesized *de novo*. To investigate the translocation of TERT to the mitochondria, we designed a fusion protein TERT-SNAP, consisting of human TERT and a SNAP-tag, a protein with the capability to selectively bind to a variety of commercially available fluorescent dyes^{16,17}. The SNAP-tag is linked to TERT from the C-terminus through a 17-amino acid linker.

To understand whether TERT is transported from the nucleus to mitochondria upon oxidative stress, we stained TERT-SNAP in transiently transfected HeLa cells with a SNAP-SiR dye. We monitored its localization in the cell before and after the induction of oxidative stress (Fig. 1A, B). Before the induction of oxidative stress, all TERT-SNAP was located within the nucleus. In the case of transport of TERT from the nucleus to the mitochondria, we expected to observe the accumulation of SNAP-SiR fluorescence in mitochondria after the induction of oxidative stress (Fig. 1A). In this experiment and all subsequent ones, oxidative stress was invoked by H₂O₂ added to the medium to concentration 500 μM, as the higher end of most oftenly used H₂O₂ concentration range for inducing oxidative stress¹⁸. Our observations indicated that 3 h after adding H₂O₂, there was no transport of TERT-SNAP to the mitochondria (Fig. 1C). All obtained images are available in Supplementary Figure S1.

TERT synthesis to mitochondria under oxidative stress

To understand whether mitochondrial TERT is synthesized *de novo* as a response to oxidative stress, we introduced an additional staining step for the TERT-SNAP following the incubation with H₂O₂ (Fig. 2A, B). In these experiments, cells expressing TERT-SNAP were stained before adding H₂O₂, the unlabeled TERT-SNAP was blocked with SNAP-Block. TERT-SNAP synthesized *de novo* was stained after the cells were incubated with H₂O₂ with a different dye (Fig. 2B). We also introduced a MitoTracker staining step to highlight the mitochondria of the cell.

Similar to our experiments described above, if mature TERT is translocated to mitochondria, the signal within mitochondria from the first dye (SNAP-505) added before the induction of oxidative stress should increase. If mitochondrial TERT is expressed *de novo* in response to oxidative stress, the fluorescence from the second dye (SNAP-SiR), added after the incubation with H₂O₂, should be detected within mitochondria. Thus, by evaluating the spectrum of the mitochondrial signal, we can gain insights into how TERT is introduced into the mitochondria under oxidative stress.

The results of the double-staining experiment were consistent with those discussed in the previous section: no discernible translocation of TERT-SNAP to mitochondria was observed. TERT-SNAP stained before the induction of oxidative stress exhibited predominant nuclear localization right before the induction of stress and 3 h after it (Fig. 2C). Unexpectedly, the second dye stained the cell cytosol rather strongly and without visible mitochondrial localization. The full image set is available in Supplementary Figure S2. An image set for a similar experiment without MitoTracker is available in Supplementary Figure S3.

To confirm these observations, we made quantitative evaluations for SNAP-505 and SNAP-SiR mitochondrial fluorescence in the double-staining experiment with MitoTracker. Although SNAP-505 exhibited some mitochondrial specificity, it didn't change significantly from 0-hour to 3-hour time points (see Supplementary Table S1). SNAP-SiR showed similar mitochondrial specificity (23% ± 8%), that is however within the scope of specificity for similarly H₂O₂-treated untransfected HeLa cells (36% ± 25%) (see Supplementary Table S2). Overall, the specificity the dyes exhibited towards mitochondria is likely connected to a weak membrane affinity of the dye, as other structures can be seen as well.

We noted that the SNAP-SiR intensity signal in the double-staining experiment was independent of whether the cell was stained with the first dye – and therefore was successfully transfected. This observation suggests nonspecific staining after the H₂O₂ incubation. We decided to conduct a control experiment to verify if that was the case.

We compared two samples of untransfected HeLa cells to check if the cells were systematically stained with SNAP-SiR after the H₂O₂ incubation. The first was simply stained with SNAP-SiR according to the protocol, and the second was incubated for 3 h in 500 μM H₂O₂, and then stained in the same manner (Fig. 3). As a result, the H₂O₂-incubated cells exhibited much higher nonspecific staining. The full image set is available in Supplementary Figure S4.

This result suggests that we might not have detected the signal from the synthesized TERT-SNAP in mitochondria due to the nonspecific cytosol labeling. To estimate this undetectable TERT-SNAP level, we obtained images of HeLa cells stained with SNAP-SiR after incubation for 3 h in 500 μM H₂O₂ and measured their cytosolic signals. We also obtained images of HeLa cells transfected with TERT-SNAP and measured their nuclear signals. We calculated the ratio between the averages of these signals (Fig. 4), which resulted in a 0,6 (± 0,24) cytosol/nuclear signal ratio. The full image set is available in Supplementary Figure S5. Assuming we

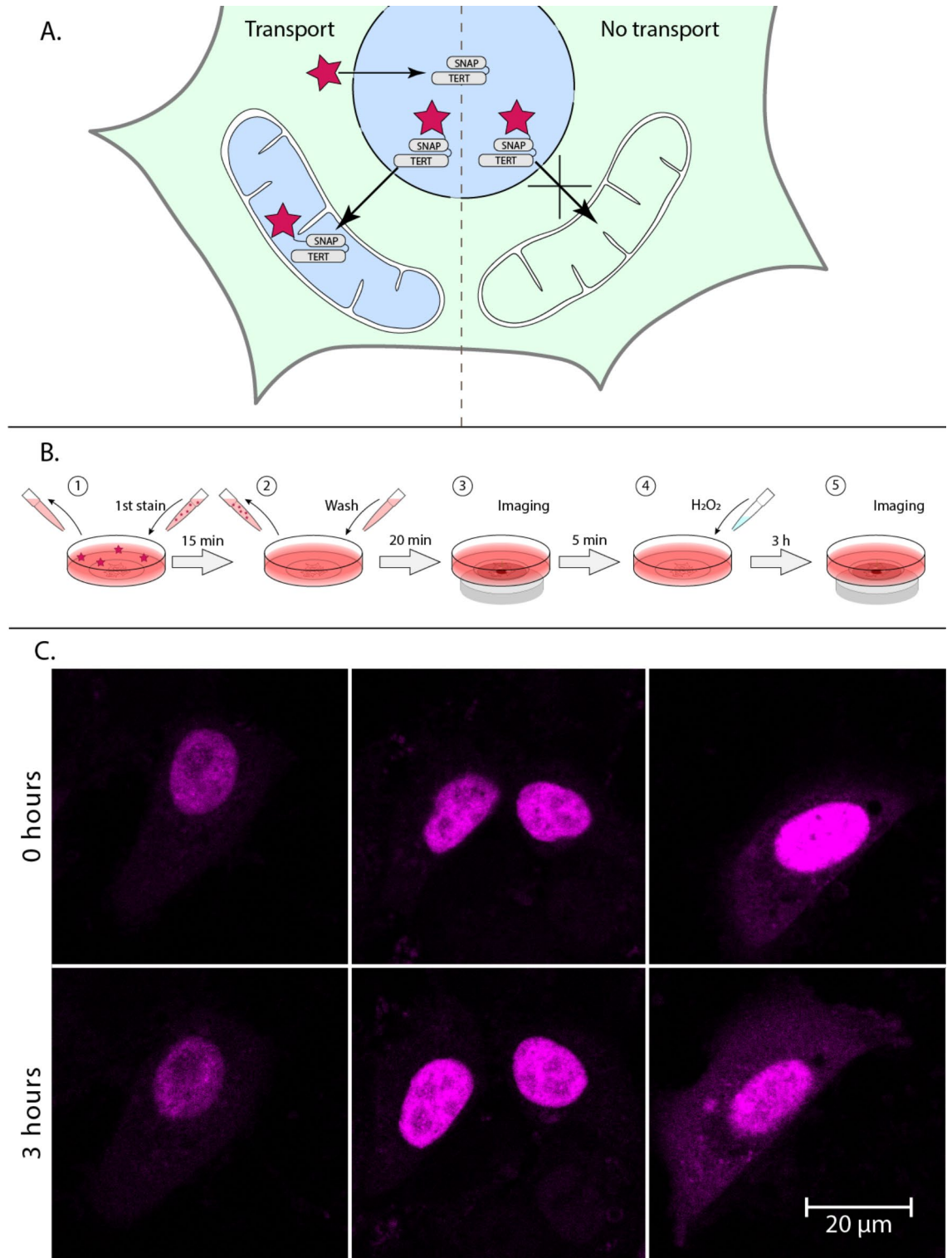


Fig. 1. TERT-SNAP transport from nucleus to mitochondria under oxidative stress. **(A)** Experimental concept: TERT-SNAP is initially confined to the cell nucleus labeled with the SNAP-specific dye (depicted as a red star). Following incubation with 500 μM H_2O_2 , two possible scenarios are depicted: left, indicating mature TERT-SNAP transport, resulting in stained mitochondria; right, suggesting the absence of transport, with non-stained mitochondria. **(B)** Experimental procedure: 1) Staining with SNAP-tag dye. 2) Washing. 3) Initial imaging. 4) Addition of H_2O_2 . 5) Subsequent imaging. **(C)** Results. Cells are stained with SNAP-SiR (shown as magenta pseudocolor), and H_2O_2 is introduced to the medium at a concentration of 500 μM . Cell images captured before H_2O_2 addition (top) and 3 hours after incubation with H_2O_2 (bottom) illustrate the absence of TERT-SNAP transport within 3 hours.

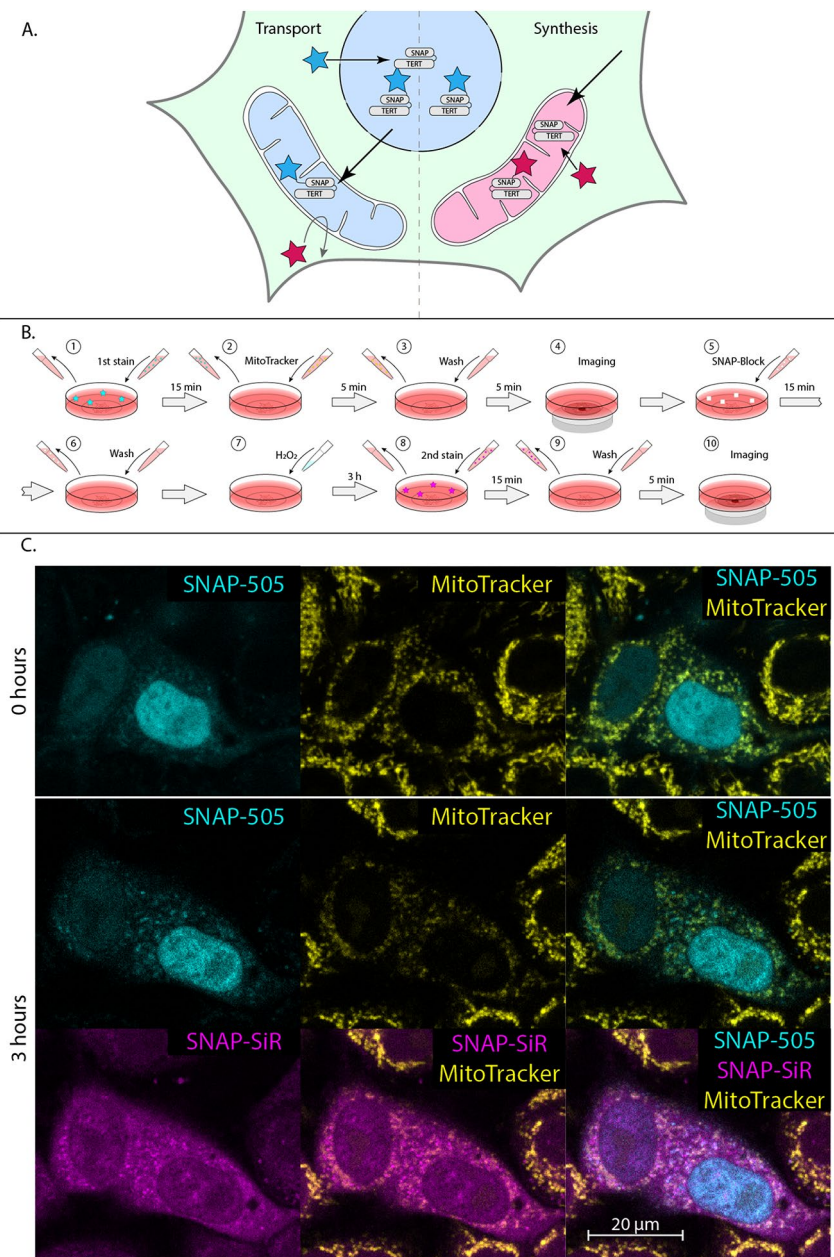


Fig. 2. TERT-SNAP synthesis into mitochondria under oxidative stress. **(A)** Experimental Concept: Before oxidative stress, TERT-SNAP is confined to the cell nucleus labeled with the first SNAP-tag specific dye (indicated as a blue star). The remaining SNAP-tag is blocked with SNAP-Block. Following incubation with 500 μM H_2O_2 , two potential outcomes are depicted: left, illustrating mature TERT-SNAP transport, leading to mitochondria containing TERT-SNAP stained with the first dye; right, representing new TERT-SNAP synthesis, with mitochondria showing no mature TERT-SNAP stained with the first dye. Instead, the second dye will stain the newly synthesized TERT-SNAP within mitochondria. **(B)** Experimental Procedure: 1) Staining with the first dye. 2) Staining with MitoTracker. 3) Washing. 4) Initial imaging. 5) Application of SNAP-Block. 6) Washing. 7) Addition of H_2O_2 . 8) Staining with the second dye after incubation. 9) Washing. 10) Subsequent imaging. **(C)** Results: Cells are stained with SNAP-505 (shown as cyan pseudocolor), and MitoTracker Red DND-99 (shown as yellow pseudocolor), while the remaining SNAP-tag is blocked with SNAP-Block. H_2O_2 is introduced to the medium to a concentration of 500 μM . After 3 hours of incubation, cells are stained with SNAP-SiR (shown as magenta pseudocolor). Consistent with previous experiments, TERT-SNAP stained before H_2O_2 addition does not appear in mitochondria. The second staining exhibits low specificity, as cells, whether stained or not with SNAP-505 (successfully transfected and not transfected), display similar signal levels from the second dye, SNAP-SiR.

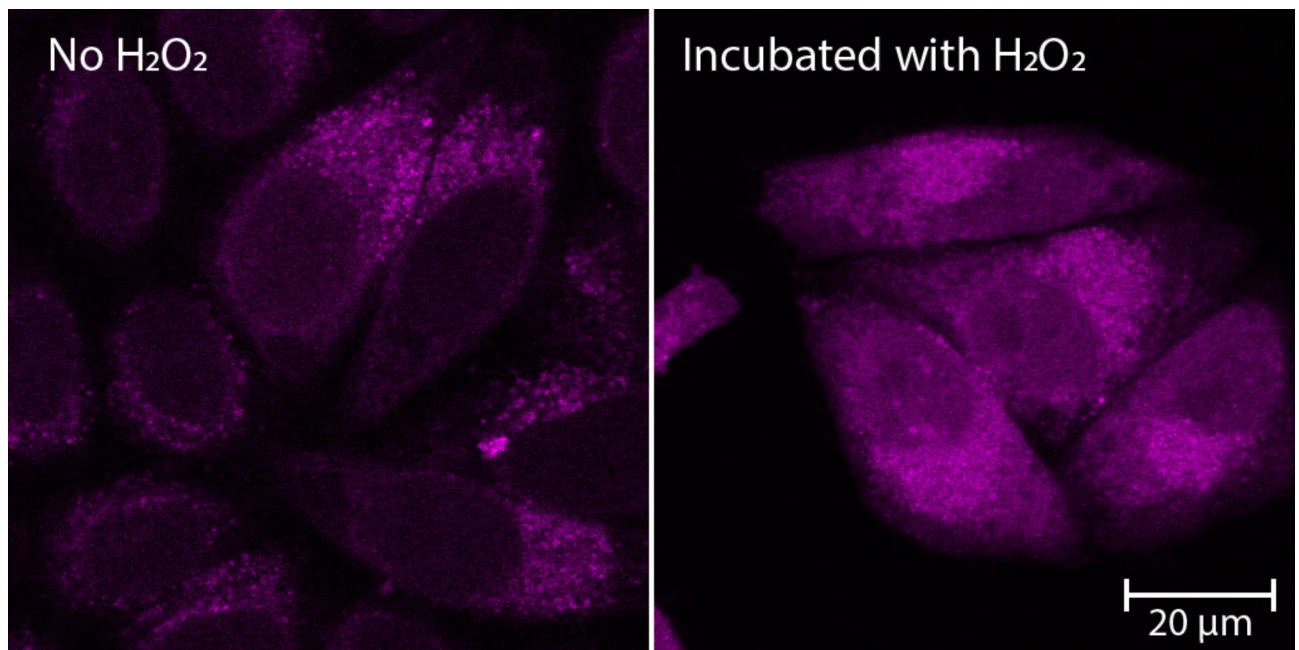


Fig. 3. Influence of H_2O_2 incubation on SNAP-Tag dye specificity. The images feature untransfected cells from two distinct dishes with untransfected HeLa cells, each stained with SNAP-SiR (shown as magenta pseudocolor) immediately before imaging. The left images feature cells untreated with H_2O_2 , while the right images depict cells incubated for 3 hours in $500 \mu\text{M}$ H_2O_2 before staining and imaging. The H_2O_2 -incubated cells exhibit high nonspecific staining.

cannot detect a fluorescent signal equal to that of the unspecific background, the undetectable threshold for TERT-SNAP fluorescent signal – and concentration – in mitochondria is roughly as high as half the nuclear concentration.

Discussion

This research aimed to investigate whether TERT is transported to the mitochondria from the nucleus or is synthesized *de novo* in response to oxidative stress. Our experiments with SNAP-tagged TERT clearly indicate the lack of mature TERT-SNAP transport from the nucleus to mitochondria. Moreover, TERT-SNAP which is potentially synthesized into mitochondria as a result of oxidative stress, remains undetected in the presence of the background fluorescent signal caused by nonspecific staining.

The quantitative approaches used in the literature for the estimation of TERT levels in mitochondria are difficult to compare with our experimental results directly. Some authors state a 1.5- or 3-fold increase in total TERT levels in mitochondria, based on Western blot¹⁵ and telomeric repeat amplification protocol (TRAP) activity measurements¹², respectively. However, as we do not see TERT in mitochondria before oxidative stress, its levels after incubation with H_2O_2 could easily be below the detectable threshold. *Singhapol et al.* employ an alternative methodology, quantifying the subcellular distribution of antibody-labeled TERT within mitochondria, asserting that approximately 40% of the overall TERT was localized in these organelles in HeLa cells following a 2-hour incubation with $400 \mu\text{M}$ H_2O_2 ¹³.

Given that mitochondria occupy 6–10% of the cell volume¹⁹ and the nucleus occupies around 40% (estimated from the measured nuclear to cytosol ratio)²⁰ in cancer cells, the fluorescence signal intensity of mitochondrial TERT can be expected to be at least three times higher than that of the nucleus. However, in our experiment, the nonspecific cytosolic signal intensity is roughly half of the nuclear signal. If this estimate is correct, the mitochondrial signal should have been detected even with the nonspecific background. It should be noted that this value is derived from several unrelated manuscripts and should therefore be considered an approximate estimate.

Another possible reason why TERT-SNAP was not detected in mitochondria is that SNAP-tag might be placing unexpected limitations on TERT transport or synthesis into mitochondria. However, our choice of SNAP-tag as the fluorescent label for our experiments was deliberate, as GFP-like proteins that are mostly used for such purposes (e.g., EmGFP, Dendra2) cannot be transported into the mitochondria in their mature state²¹. This limitation is attributed to the structural characteristics of these proteins, particularly their β -barrel form being unable to be unfolded by the mitochondrial transport machinery. In contrast, mature SNAP-tag can be effectively transported into the mitochondrial matrix, even when bound to a SNAP-tag dye. The transport signaling appears unaffected, as the SNAP-tag was positioned on the C-terminus of TERT, whereas the MTS in TERT is situated on the N-terminus. Given these considerations, SNAP-tag is unlikely to prevent TERT-SNAP from being transported into the mitochondria by the mitochondrial transport machinery.

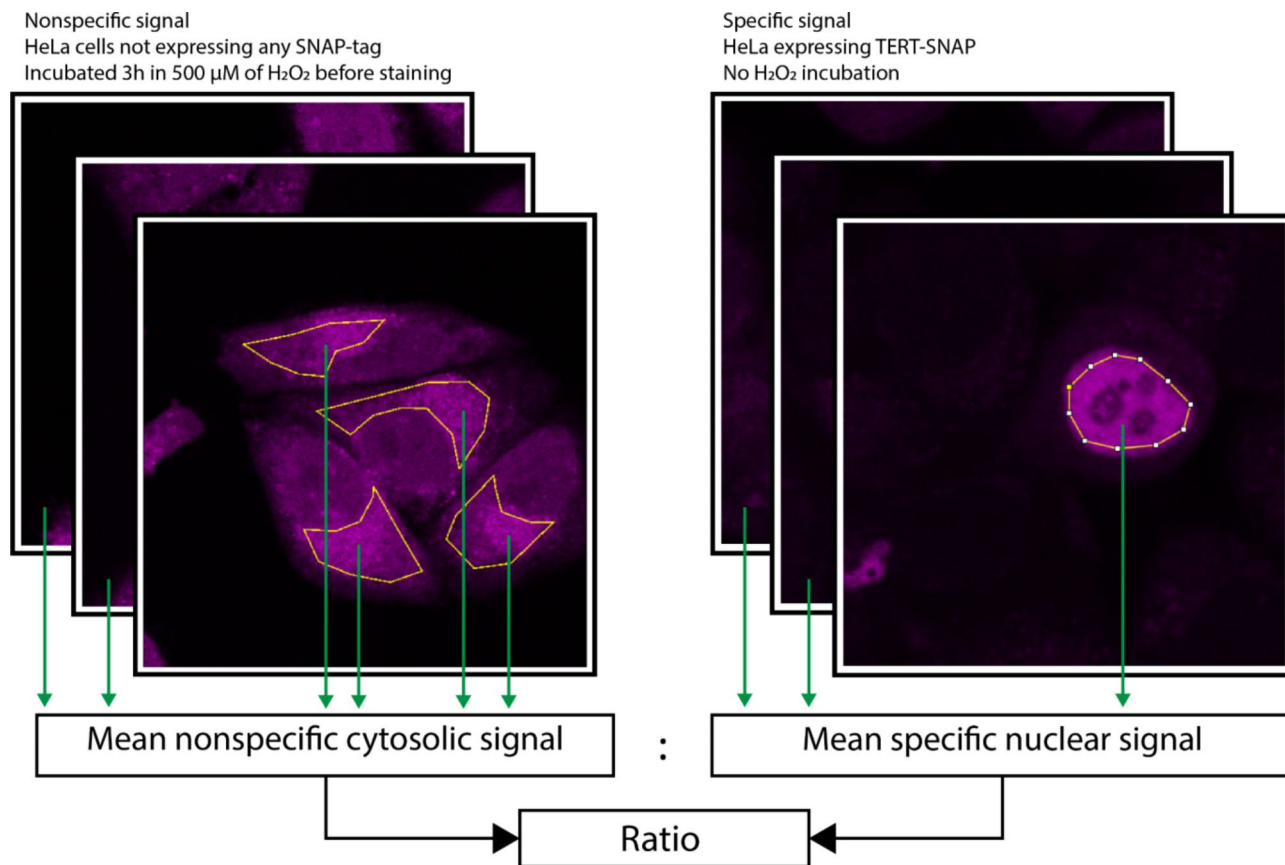


Fig. 4. Nonspecific fluorescence due to H_2O_2 incubation evaluation. SNAP-SiR signals (shown as magenta pseudocolor) were derived from cells with nonspecifically stained cytosols (left, not transfected, incubated with H_2O_2) and specifically stained nuclei (right, transfected, not incubated with H_2O_2). Mean cytosolic and nuclear signals were found, and the ratio between them was calculated.

It is, however, possible that SNAP-tag attachment to the C-terminus has disrupted the redistribution of TERT-SNAP. The nuclear export of TERT is regulated by CRM1 that binds to the TERT nuclear export signal²². This process is inhibited by a 14-3-3 protein binding to an FKT sequence at 1127 position²³, thus promoting TERT export from the nucleus. This FKT sequence is only 3 amino acids apart from the C-terminal end of TERT. SNAP-tag may be interfering with the 14-3-3 binding site in a manner that results in blocking TERT-SNAP nuclear export. In this case, future fluorescent tagging of TERT requires significant reordering of chimeric construct to avoid interference with multiple transport signals existing in TERT.

Materials and methods

Cell culture

All experiments were conducted on HeLa cells. The HeLa cell line was kindly gifted by the Laboratory of cell interactions of the Shemyakin and Ovchinnikov Institute of Bioorganic Chemistry (Russian Academy of Sciences). Cells were cultivated in DMEM (Gibco, USA) supplemented with 10% FBS (Cytiva, USA), 1% Pen-Strep (Gibco, USA), 1% GlutaMax (Gibco, USA), 10 mM HEPES (Gibco, USA), cultivated in Galaxy 170R incubator (Eppendorf, Germany) at 37 °C, 100% humidity, and 5% CO_2 to maintain culture pH.

TERT-SNAP cell transfection

The transfection of HeLa cells was performed with a plasmid pcDNA TERT-SNAP using the Effectene (QiaGen) kit according to the manufacturer's instructions. Cells were transfected transiently, without selection, one day prior to reseeding to the dish, with transfection efficiency ranging from 4 to 15%.

The pcDNA TERT-SNAP plasmid was created on the basis of pcDNA 3.1 (+) vector. It contains a gene encoding fused proteins human TERT and SNAP-tag, connected with a 17-amino acid linker (KLRILQSTVPRARDPPV) (Scheme in Supplementary Figure S6). The linker length was chosen to reduce both potential interactions between TERT and SNAP-tag and to avoid SNAP-tag mitochondrial import with SNAP-tag resting outside²⁴. The gene is expressed under a CMV promoter.

Oxidative stress assay

To cause oxidative stress in cells, H_2O_2 was added to complete medium to concentration 500 μM . To assure that the cells are under the effect of oxidative stress, two experiments were performed.

In the first experiment, cells were seeded into four 35 mm dishes, 80,000 to each, and incubated overnight. The next day H_2O_2 was added to the dishes, to concentrations (0, 200, 500 and 1000 μM). The cells were incubated for 30 min, then washed with PBS and detached with TripleE. Then they were detached with DMEM and centrifuged (200 g, 5 min), then the medium was replaced with warmed 0,5 ml of HBSS. MitoSOX Red was added to concentration 2 μM to the samples. All the samples were incubated for 30 min at 37 °C. All the samples were then centrifuged, washed with PBS, centrifuged again and washed with 100 μL of 1x Buffer for Annexin-V-FITC (Lumiprobe). The cells were centrifuged, the old buffer was replaced with a new 100 μL of 1x Buffer. 2 μL of Annexin-V stock solution was added to each probe. The cells were incubated at room temperature for 15 min. Then 400 μL of 1x Buffer was added, the cells were incubated for 5 min, and measured with a flow cytometer Accuri C6. Living cells were identified on the FSC-SSC channel diagram, and apoptotic cells were excluded on the FL1-FSC diagram. FL-2 (MitoSOX signal) histograms were compared. According to the histograms, H_2O_2 was influencing the FL-2 signal in a concentration-dependent manner (Supplementary Figure S7 A).

In the second experiment, the cells were seeded into four 35 mm dishes, 80,000 to each, and incubated overnight. The next day H_2O_2 was added to the dishes, to concentrations (0, 200, 500 and 1000 μM). The cells were incubated for 30 min, then washed with PBS, and the medium was replaced with 0,5 ml of HBSS, with 2 μM MitoSOX Red. The cells were incubated with MitoSOX for 30 min, then washed with PBS and observed with fluorescent microscopy methods. As in the previous experiment, H_2O_2 was influencing the FL-2 signal in a concentration-dependent manner (Supplementary Figure S7 B).

Fluorescence microscopy

Imaging was conducted on LSM780 (Zeiss, Germany) microscope, using an oil immersion 100x NA = 1.46 objective (Objective alpha Plan-Apochromat 100x/1.46 Oil DIC M27). For dye excitation the following lasers were used: 488 nm for 505-SNAP and MitoTracker Orange, 561 nm for TMR-Star, 633 nm for SNAP-SiR, utilizing dichroics MBS 488, MBS 488/561 and MBS 488/561/633. The fluorescence was detected with a QUASAR detector in a spectral-resolved mode with 9 nm spectral resolution in the 494–690 nm range. After the imaging, the signals from several dyes were separated using the Linear Unmixing tool (ZEN). During the experiment, the cells were kept in InuBG2H-Ely incubator (TOKAI HIT, Japan) maintaining temperature of 37 °C, 100% humidity and 5% CO_2 concentration.

To track TERT-SNAP transport into mitochondria, 80,000 transfected HeLa cells expressing TERT-SNAP were seeded on a μ -Dish 35 mm, Grid-500 ibiTreat (Ibidi) the day before the experiment. Cells were stained with SNAP-SiR (NEB) according to the manufacturer's instructions. This dye is membrane-permeable and is designed to stain SNAP-tag inside living cells. After the staining process, H_2O_2 was added to a concentration of 500 μM in the medium to cause oxidative stress. The cells were incubated for 3 h. Cell images were obtained during the experiment before H_2O_2 addition and after 3 h of incubation with H_2O_2 .

To track TERT-SNAP synthesis into mitochondria, 80,000 transfected HeLa cells expressing TERT-SNAP were seeded on a μ -Dish 35 mm, Grid-500 ibiTreat (Ibidi) the day before the experiment. The experiment was conducted twice: with and without MitoTracker. In the first case, the cells were subsequently stained with 505-Star and MitoTracker Orange, and the remaining mature SNAP-tag was blocked with SNAP-Block (Neb). In the second case, the cells were stained with TMR-Star, and all remaining SNAP-tag was blocked with SNAP-Block. In both cases, SNAP-Block is required to block all mature TERT-SNAP that was produced before oxidative stress, to prevent its binding with the second stain (see a similar experiment results without SNAP-Block in Supplementary Figures S8 and S9). After the incubation with SNAP-Block, H_2O_2 was added to a concentration of 500 μM in the medium to cause oxidative stress. The cells were incubated for 3 h and then stained with SNAP-SiR. All used dyes and SNAP-Block are membrane-permeable and are designed to stain or block SNAP-tag inside living cells. Cell images were obtained twice during the experiment: before adding SNAP-Block and after incubation with H_2O_2 .

To specify the influence of H_2O_2 incubation with cells on nonspecific cytosol staining, 80,000 transfected and 80,000 untransfected HeLa cells were seeded on two separate 35 mm μ -Dishes (ibidi) the day before the experiment. The transfected cells were stained with SNAP-SiR in an ordinary manner. Untransfected cells were incubated in DMEM with 500 μM H_2O_2 for 3 h, then washed and stained with SNAP-SiR. Cell images from each dish were obtained. Mean signal from the nucleus of each transfected cell (9 cells total) from the 1st image set (transfected cells) was derived. The mean signal from the cytosol of each cell (27 cells total) was derived from the 2nd image set (untransfected cells). The cytosolic and nuclear signals were averaged separately by the dataset, and the ratio between the average nonspecific cytosolic signal and average specific nuclear signal was found.

Negative controls were performed for each dye in each experiment by staining untransfected HeLa cells and obtaining their images under the same conditions.

Image processing

To make quantitative evaluations for the dyes' level in the cellular compartments in the double-staining experiment with MitoTracker, the following procedure was used. Mitochondrial region on the image was selected using the Auto Local Threshold²⁵ plugin in FIJI²⁶. Another area representing the whole cell without the nucleus was selected manually. Combining these two areas, two other selections were created: the mitochondria of the cell, and the cytoplasm of the cell without the mitochondria. In these areas, mean dye signals were measured. A graphical representation can be found in Supplementary Figure S10.

For SNAP-505, the ratio between the mitochondrial and cytoplasmic signals was calculated for each cell in the double-staining experiment with MitoTracker, before and after H_2O_2 incubation. We chose to track this ratio, as it would account for protein turnover and bleaching. For each individual cell, a ratio between these ratios was calculated (post- H_2O_2 incubation to pre- H_2O_2 incubation). For this parameter, representing the change in mitochondrial SNAP-505 specificity, the mean value with standard deviation was found.

For SNAP-SiR, the ratio between the mitochondrial and cytoplasmic signals was calculated for each cell in the double-staining experiment with MitoTracker after H₂O₂ incubation. As we are unable to compare the signal from the 2nd staining for the same cells at different moments, the cells from the double-staining experiment were compared to untransfected cells, also incubated with H₂O₂ (same concentration and incubation time) and stained with SNAP-SiR. Mean and standard deviation of the mitochondria-to-cytoplasm signal ratios were calculated for the transfected and untransfected cells.

Data availability

Data is provided within the manuscript or supplementary information files.

Received: 27 February 2024; Accepted: 1 October 2024

Published online: 15 October 2024

References

- Chan, S. R. W. L. & Blackburn, E. H. Telomeres and telomerase. *Philos. Trans. R Soc. Lond. B Biol. Sci.* **359**, 109–121 (2004).
- Zheng, Q., Huang, J. & Wang, G. Mitochondria, telomeres and telomerase subunits. *Front. Cell. Dev. Biol.* **7**, 274 (2019).
- Gazzaniga, F. S. & Blackburn, E. H. An antiapoptotic role for telomerase RNA in human immune cells independent of telomere integrity or telomerase enzymatic activity. *Blood*. **124**, 3675–3684 (2014).
- Eitan, E. et al. Expression of functional alternative telomerase RNA component gene in mouse brain and in motor neurons cells protects from oxidative stress. *Oncotarget*. **7**, 78297–78309 (2016).
- Liu, H., Yang, Y., Ge, Y., Liu, J. & Zhao, Y. TERC promotes cellular inflammatory response independent of telomerase. *Nucleic Acids Res.* **47**, 8084–8095 (2019).
- Udroiu, I., Marinaccio, J. & Sgura, A. Many functions of Telomerase Components: certainties, doubts, and inconsistencies. *Int. J. Mol. Sci.* **23**, 15189 (2022).
- Maida, Y. et al. An RNA-dependent RNA polymerase formed by TERT and the RMRP RNA. *Nature*. **461**, 230–235 (2009).
- Sharma, N. K. et al. Human telomerase acts as a hTR-independent reverse transcriptase in mitochondria. *Nucleic Acids Res.* **40**, 712–725 (2012).
- Santos, J. H., Meyer, J. N., Skorvaga, M., Annab, L. A. & Van Houten, B. Mitochondrial hTERT exacerbates free-radical-mediated mtDNA damage. *Aging Cell*. **3**, 399–411 (2004).
- Haendeler, J. et al. Mitochondrial telomerase reverse transcriptase binds to and protects mitochondrial DNA and function from damage. *Arterioscler. Thromb. Vasc. Biol.* **29**, 929–935 (2009).
- Santos, J. H., Meyer, J. N. & Van Houten, B. Mitochondrial localization of telomerase as a determinant for hydrogen peroxide-induced mitochondrial DNA damage and apoptosis. *Hum. Mol. Genet.* **15**, 1757–1768 (2006).
- Ahmed, S. et al. Telomerase does not counteract telomere shortening but protects mitochondrial function under oxidative stress. *J. Cell. Sci.* **121**, 1046–1053 (2008).
- Singhapol, C. et al. Mitochondrial telomerase protects cancer cells from nuclear DNA damage and apoptosis. *PLoS ONE*. **8**, e52989 (2013).
- Haendeler, J., Hoffmann, J., Brandes, R. P., Zeiher, A. M. & Dimmeler, S. Hydrogen peroxide triggers nuclear export of telomerase reverse transcriptase via src kinase family-dependent phosphorylation of tyrosine 707. *Mol. Cell. Biol.* **23**, 4598–4610 (2003).
- Marinaccio, J. et al. TERT extra-telomeric roles: antioxidant activity and mitochondrial protection. *Int. J. Mol. Sci.* **24**, 4450 (2023).
- Cole, N. B. Site-specific protein labeling with SNAP-tags. *Curr. Protoc. Protein Sci.* **73**, 30.1.1–30.1.16 (2013).
- Keppler, A. et al. A general method for the covalent labeling of fusion proteins with small molecules in vivo. *Nat. Biotechnol.* **21**, 86–89 (2003).
- Ransy, C., Vaz, C., Lombès, A. & Bouillaud, F. Use of H₂O₂ to cause oxidative stress, the Catalase Issue. *Int. J. Mol. Sci.* **21**, 9149 (2020).
- Vazquez, A. *Overflow Metabolism: from Yeast to Marathon Runners* (Elsevier Science, 2017).
- Moore, M. J., Sebastian, J. A. & Kolios, M. C. Determination of cell nucleus-to-cytoplasmic ratio using imaging flow cytometry and a combined ultrasound and photoacoustic technique: a comparison study. *J. Biomed. Opt.* **24**, 1–10 (2019).
- Bogorodskiy, A. et al. Accessing mitochondrial protein import in living cells by protein microinjection. *Front. Cell. Dev. Biol.* **9**, 698658 (2021).
- Seimiya, H. et al. Involvement of 14-3-3 proteins in nuclear localization of telomerase. *EMBO J.* **19**, 2652–2661 (2000).
- Banik, S. S. R. et al. C-terminal regions of the human telomerase catalytic subunit essential for in vivo enzyme activity. *Mol. Cell. Biol.* **22**, 6234–6246 (2002).
- Rassow, J., Hartl, F. U., Guiard, B., Pfanner, N. & Neupert, W. Polypeptides traverse the mitochondrial envelope in an extended state. *FEBS Lett.* **275**, 190–194 (1990).
- Auto Local Threshold. *ImageJ Wiki* <https://imagej.net/plugins/auto-local-threshold>
- Schindelin, J. et al. Fiji: an open-source platform for biological-image analysis. *Nat. Methods*. **9**, 676–682 (2012).

Acknowledgements

V.B., A.B., I.M., E.S., N.I. and D.B. acknowledge the Ministry of Science and Higher Education of the Russian Federation (agreement # 075-03-2024-117, project FSMG-2024-0012, for experiments on TERT transport to mitochondria); R.N. acknowledges the Ministry of Science and Higher Education of the Russian Federation (State Task 075-03-2024-117, Project No. FSMG-2023-0015, for experiments on TERT synthesis to mitochondria); S.L. acknowledges the Russian Science Foundation (project (No. 23-14-00220) for experiments on TERT synthesis to mitochondria). O.M. acknowledges the Russian Science Foundation (project 22-74-10036, <https://rscf.ru/project/22-74-10036/>, for cell preparation and support). The authors would like to thank Joachim Altschmied and Judith Haendeler for providing the human TERT coding sequence, their support and scientific discussion during the project.

Author contributions

D.B. wrote the initial draft and performed the microscopy experiments. D.B., A.B., I.M., T.G. and V.B. introduced the research concept. D.B., A.B., I.M. and N.I. designed the experiment methodology. O.M. performed the cell cultivation and transfection. E.S. validated the results. R.N., S.L., G.B. and V.G. provided the necessary reagents and equipment. S.L. and V.B. acquired the funding for the project. A.M., V.G. and V.B. provided administrative support. A.B., V.B. supervised the project. All authors contributed to editing the manuscript.

Funding

This work was supported by the Ministry of Science and Higher Education of the Russian Federation (agreement # 075-03-2024-117, project FSMG-2024-0012, for experiments on TERT transport to mitochondria) for V.B., A.M., A.B., E.S., D.B. and N.I.; (State Task 075-03-2024-117, Project No. FSMG-2023-0015, for experiments on TERT synthesis to mitochondria) for R.N.; the Russian Science Foundation (project (No. 23-14-00220) for experiments on TERT synthesis to mitochondria) for S.L; and (project 22-74-10036, <https://rscf.ru/project/22-74-10036/>, for cell preparation and support) for O.M.

Declarations

Competing interests

The authors declare no competing interests.

Additional information

Supplementary Information The online version contains supplementary material available at <https://doi.org/10.1038/s41598-024-75127-4>.

Correspondence and requests for materials should be addressed to V.B.

Reprints and permissions information is available at www.nature.com/reprints.

Publisher's note Springer Nature remains neutral with regard to jurisdictional claims in published maps and institutional affiliations.

Open Access This article is licensed under a Creative Commons Attribution-NonCommercial-NoDerivatives 4.0 International License, which permits any non-commercial use, sharing, distribution and reproduction in any medium or format, as long as you give appropriate credit to the original author(s) and the source, provide a link to the Creative Commons licence, and indicate if you modified the licensed material. You do not have permission under this licence to share adapted material derived from this article or parts of it. The images or other third party material in this article are included in the article's Creative Commons licence, unless indicated otherwise in a credit line to the material. If material is not included in the article's Creative Commons licence and your intended use is not permitted by statutory regulation or exceeds the permitted use, you will need to obtain permission directly from the copyright holder. To view a copy of this licence, visit <http://creativecommons.org/licenses/by-nc-nd/4.0/>.

© The Author(s) 2024